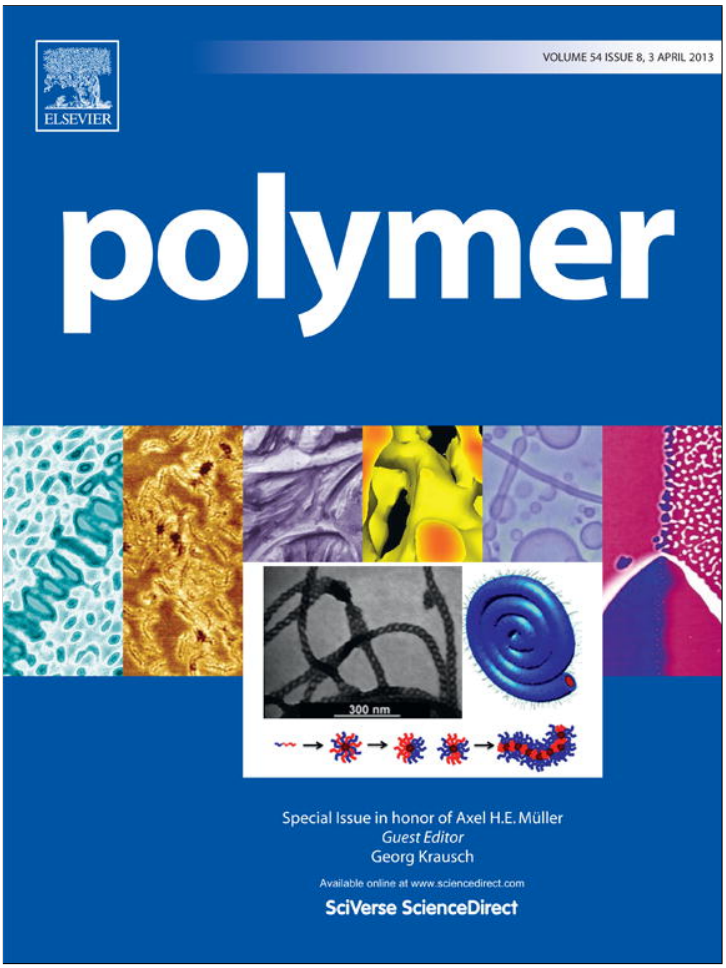

Polymer 54 (2013) 2115–2122

Contents lists available at SciVerse ScienceDirect

Polymer

journal homepage: www.elsevier.com/locate/polymer

Facile preparation of photodegradable hydrogels by photopolymerization

Chang Seok Ki, Han Shih, Chien-Chi Lin*

Department of Biomedical Engineering, Purdue School of Engineering and Technology, Indiana University-Purdue University at Indianapolis, Indianapolis, IN 46202, USA

ARTICLE INFO

Article history:
Received 29 November 2012
Received in revised form
31 January 2013
Accepted 11 February 2013
Available online 18 February 2013

Keywords:
Photopolymerization
Photodegradable hydrogels
Click reaction

ABSTRACT

Photodegradable hydrogels have emerged as a powerful material platform for studying and directing cell behaviors, as well as for delivering drugs. The premise of this technique is to use a cytocompatible light source to cleave linkers within a hydrogel, thus causing reduction of matrix stiffness or liberation of matrix-tethered biomolecules in a spatial-temporally controlled manner. The most commonly used photodegradable units are molecules containing nitrobenzyl moieties that absorb light in the ultraviolet (UV) to lower visible wavelengths (~280–450 nm). Because photodegradable linkers and hydrogels reported in the literature thus far are all sensitive to UV light, highly efficient UV-mediated photopolymerizations are less likely to be used as the method to prepare these hydrogels. As a result, currently available photodegradable hydrogels are formed by redox-mediated radical polymerizations, emulsion polymerizations, Michael-type addition reactions, or orthogonal click chemistries. Here, we report the first photodegradable poly(ethylene glycol)-based hydrogel system prepared by step-growth photopolymerization. The model photolabile peptide cross-linkers, synthesized by conventional solid phase peptide synthesis, contained terminal cysteines for step-growth thiol-ene photo-click reactions and a UV-sensitive 2-nitrophenylalanine residue in the peptide backbone for photo-cleavage. Photolysis of this peptide was achieved through adjusting UV light exposure time and intensity. Photopolymerization of photodegradable hydrogels containing photolabile peptide cross-linkers was made possible via a highly efficient visible light-mediated thiol-ene photo-click reaction using a non-cleavage type photoinitiator eosin-Y. Rapid gelation was confirmed by *in situ* photo-rheometry. Flood UV irradiation at controlled wavelength and intensity was used to demonstrate the photodegradability of these photopolymerized hydrogels.

1. Introduction

Hydrogels containing photodegradable linkers have great potential in controlled release and tissue engineering applications [1]. For example, drugs or cells immobilized or entrapped within a photodegradable hydrogel can be released 'on-demand' via light-mediated cleavage of photolabile linkers [2–5]. Furthermore, the cleavage of photolabile cross-links leads to the reduction of hydrogel cross-linking density and stiffness [1,6,7]. This approach has been used to study cell fate processes, such as migration of fibroblast [1], de-activation of valvular interstitial cells (VICs) [7,8], and differentiation of human mesenchymal stem cells (hMSCs) [1]. Most of the photolabile units contain an *ortho*-nitrobenzyl (*o*-NB) moiety, which is highly susceptible to ultraviolet (UV) light exposure. The absorbance spectra of macromers containing *o*-NB groups usually peak at around 280–400 nm and tail off in the lower visible light range (~430 nm) [2,5]. When exposing to lights at selective wavelengths, *o*-NB groups are effectively photo-lysed, resulting in the liberation of conjugated molecules or reduction in gel cross-linking density.

The exploration of photodegradable hydrogels thus far has focused on synthesizing photolabile groups with different light sensitivities or on controlling cellular response via photolysis-induced material property changes. Current methods to fabricate photodegradable hydrogels are restricted to non-photo-mediated reactions, such as Michael-type conjugations, redox reactions, emulsion polymerization, thermal polymerizations, or orthogonal 'click' chemistries [1,9–16]. While these gelation schemes preserve the molecular integrity of photodegradable moieties, some limitations exist. For example, redox radical polymerizations compatible with photolabile units are commonly initiated by cytotoxic components such as ammonium persulfate (APS) and tetramethylethylenediamine (TEMED) [9,12,17]. Although gels prepared from Michael-type addition reactions contain no cytotoxic components, this reaction scheme suffers from low functional group conversion and long gelation time due to significant intramolecular reactions [18–20]. Alternatively, researchers have begun to use cytocompatible orthogonal 'click' chemistries, such as the copper-

* Corresponding author.
E-mail address: lincc@iupui.edu (C.-C. Lin).

0032-3861/$ – see front matter © 2013 Elsevier Ltd. All rights reserved.
http://dx.doi.org/10.1016/j.polymer.2013.02.018

free strain-promoted azide-alkyne cycloaddition reaction, to synthesize photo-tunable hydrogels [13,21–23]. However, none of the above cross-linking methods permit spatial-temporal controls during gelation because the polymerization starts as soon as the macromers are mixed together.

Photopolymerization has always been one of the most popular methods to fabricate hydrogels due to rapid and highly tunable gelation kinetics. This attractive gelation method, however, is unfortunately excluded from the polymerization of photodegradable hydrogels. We hypothesized that photodegradable hydrogels can be synthesized by photopolymerization if an appropriate and efficient photopolymerization system is available. Our laboratory has recently reported the synthesis of step-growth hydrogels by visible light-mediated thiol-ene photo-click reactions [24]. A halogen cold light lamp was used as a cytocompatible visible light source while eosin-Y (EY) was used as the sole initiator to initiate thiol-ene photo-click gelation using macromer poly(ethylene glycol)-tetra-norbornene (PEG4NB) and cross-linker dithiothreitol (DTT). This new step-growth hydrogel system not only preserves all favorable features offered by the rapid and tunable photochemistry, but also excludes the use of potentially cytotoxic components (e.g., triethanolamine) that are indispensable in the conventional visible light-mediated chain-growth photopolymerizations. We reasoned that this new photopolymerization scheme (Scheme 1A) could be used to synthesize photodegradable hydrogels since the absorbance of eosin-Y peaks at around 516 nm, a wavelength far away from the absorbance of all reported photolabile *o*-NB groups [1–3,5].

In this contribution, we report a proof-of-principle photopolymerization system using orthogonal wavelengths that are compatible for forming photodegradable hydrogels. A simple yet highly efficient visible light-mediated thiol-ene photo-click reaction was utilized to fabricate step-growth photodegradable hydrogels cross-linked by PEG4NB and a photolabile peptide containing a commercially available photolabile amino acid, L-2-nitrophenylalanine (NPA) (Scheme 1B). The model peptide Cys–Gly–NPA–Gly–Cys (CGOGC, O: NPA residue. Cysteines were added for thiol-ene photo-crosslinking) was synthesized by standard solid phase peptide synthesis (SPPS) while the formation of hydrogels was accomplished within minutes using a halogen cold light lamp that emits bright visible light. The photodegradation of these photopolymerized hydrogels was achieved by flood UV light irradiation.

2. Experimental section

2.1. Materials

4-arm PEG (20 kDa) was purchased from JenKem Technology USA. Fmoc-Rink Amide MBHA resin, Fmoc-Cys(Trt)-OH, Fmoc-Gly-OH, Fmoc-Tyr(tBu)-OH, and reagents for peptide synthesis were acquired from Chempep, Inc. Fmoc-L-2-nitrophenylalanine-OH (Fmoc-2-NPA) was obtained from PepTech Inc. HPLC grade acetonitrile and water were obtained from Fisher Scientific and VWR International, respectively. Eosin-Y disodium salt was acquired from Fisher Scientific. All other chemicals and reagents were obtained from Sigma–Aldrich unless otherwise noted.

2.2. Macromer and peptide synthesis

PEG-tetra-norbornene (PEG4NB) and photoinitiator lithium arylphosphinate (LAP) were synthesized as described previously [25,26] and characterized by ^{1}H NMR (85–95%). Photolabile peptides (NH_2-CGOGC-NH_2 and Ac-CGOGC-NH_2) and non-photolabile peptides (NH_2-CGGGC-NH_2 and NH_2-CGGYC-NH_2) were synthesized using Fmoc-Rink-Amide HBMA resin in a microwave-assisted solid peptide synthesizer (CEM Discover SPS) following standard HOBT/HBTU coupling chemistry. Deprotection of Fmoc groups and coupling of Fmoc-amino acids (with the exception of Fmoc-Cys(Trt)-OH) were performed at 50 W, 75 °C for 3 and 5 min, respectively. Coupling of Fmoc-Cys(Trt)-OH was performed at 50 W, 50 °C for 10 min to reduce racemization. A portion of CGOGC was acetylated by reacting peptide N-terminus with acetic anhydride (0.5 M acetic anhydride and 0.125 M diisopropylethylamine in dimethylformamide) before cleavage using a cleavage cocktail (95% trifluoroacetic acid, 2.5% dH_2O, 2.5% triisopropylsilane, and 5 wt/vol % phenol). Crude peptides were purified by reverse phase HPLC (RP-HPLC, Perkin Elmer Flexar system) to at least 95% purity. The purified peptides were characterized by mass spectrometry (Agilent Technology).

2.3. Characterization of photodegradable peptides

UV/Vis absorbance spectra of the photoinitiators (eosin-Y (EY) and lithium arylphosphinate (LAP)) and photodegradable peptides (NH_2-CGOGC-NH_2 and Ac-CGOGC-NH_2) were measured using a

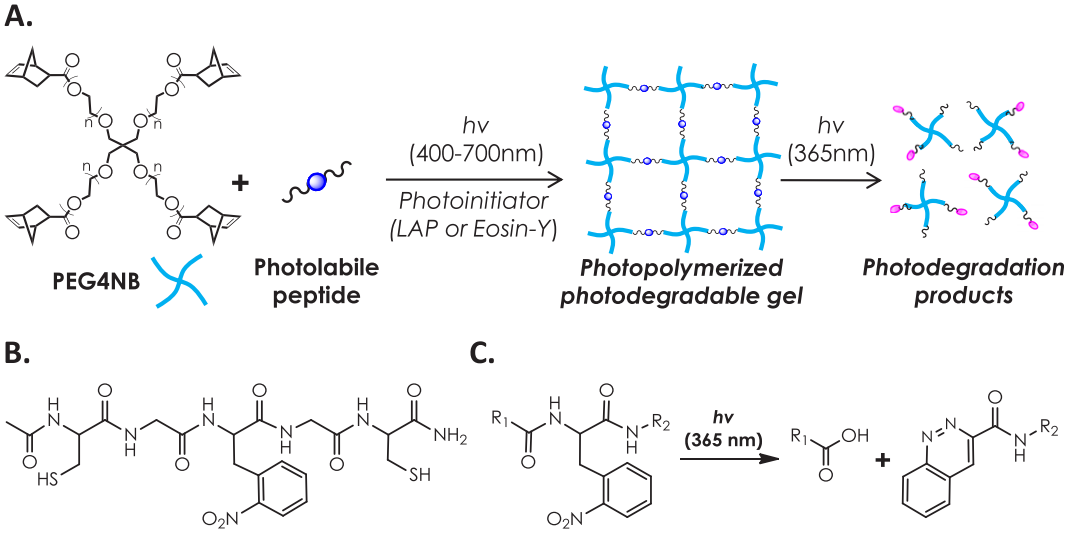

Scheme 1. (A) Schematic of photo-crosslinking and photodegradation of step-growth thiol-ene hydrogels. (B) Chemical structure of model photodegradable peptide Ac-CGOGC-NH_2. (C) Schematic of UV-mediated peptide photolysis.

microplate reader (BioTek Synergy HT). The peptides were dissolved in 10% (v/v) dimethylsulfoxide (DMSO) aqueous solution for increasing the peptide solubility. Beer's Law was employed to convert the absorbance into molar absorbability. For the solution turbidity measurement, 8 mM Ac-CGOGC-NH_2 in 10% (v/v) DMSO aqueous solution was exposed to UV light (10 mW/cm^2, 365 nm) in a closed glass tube for 30 min. Its optical absorbance at 700 nm was measured by using a microplate reader and the turbidity was determined by following equation [27].

$$\text{Turbidity}\left(\text{cm}^{-1}\right) = \frac{-\ln(\text{Transmittance at 700 nm})}{\text{Path length(cm)}}$$

To characterize the photodegradation kinetics of the peptide, NH_2-CGOGC-NH_2 and Ac-CGOGC-NH_2 were dissolved in distilled water and 10% (v/v) DMSO aqueous solution, respectively. 500 μl solution was added in a closed glass tube (outer diameter: 9.75 mm, wall thickness: 0.625 mm) and exposed to UV light source (Omnicure S1000) at 365 nm through a liquid light guide. The glass tube and light source were positioned so that the vertical axis of the glass tube and light path were perpendicular. The light intensity was measured at the identical distance from the light source to the center of the solution. Analytical RP-HPLC and ^{1}H NMR were used to evaluate photolysis products. For RP-HPLC, the photodegraded samples were passed through 0.2 μm PVDF filters to remove insoluble precipitates prior to injection into the HPLC column. For ^{1}H NMR analysis, 10 mg Ac-CGOGC-NH_2 was dissolved in 400 μl 10% methyl sulfoxide-d6/90% deuterium oxide and exposed to UV light (10 mW/cm^2, 365 nm) for 20 min ^{1}H NMR spectra were obtained by a NMR spectrometer (500 MHz Avance III, Bruker).

2.4. Photopolymerization and photodegradation of hydrogels

Step-growth thiol-norbornene hydrogels were synthesized using PEG4NB and CGOGC (amine-terminated or acetylated) at a unity stoichiometric ratio between the norbornene and thiol moieties. A UV/IR filter was installed between the halogen cold light lamp (AmScope Inc.) and the macromer solution to ensure the transmission of lights at the visible wavelengths (400–700 nm). Photoinitiator EY (0.1 mM) or LAP (1 mM) was used to initiate photopolymerization upon visible light exposure (70,000 Lux). Gelation (5 wt% PEG4NB and NH_2-CGOGC-NH_2) was monitored by *in situ* photo-rheometry in a CVO digital rheometer (Malvern) using the same halogen light source connected to a light cure cell. Time sweep oscillatory rheometry was operated at 1 Hz frequency and 10% strain. Light was turned on 30 s after the onset of rheometrical measurement. Gel points were determined by identifying the crossover time when the elastic modulus (G′) surpasses viscous modulus (G″).

Hydrogel samples for photodegradation studies were prepared using 8 wt% PEG4NB and Ac-CGOGC-NH_2 with 0.1 mM EY in between two cover glasses separated by 1 mm thick spacers. Non-photo-cleavable peptides (e.g., CGGGC and CGGYC) were used in control experiments. Following gelation, the hydrogel was equilibrated in distilled water for 24 h and circular gel discs were obtained using an 8 mm (dia.) biopsy punch. The hydrogel samples were exposed to UV light (302 or 365 nm) for photodegradation. During UV exposure, the gel samples were kept in distilled water to prevent drying. The residual mass of the gel sample was measured gravimetrically after removing excess water on the gel surface with Kimwipe tissue.

2.5. Statistics

Student's *T*-test was performed to assess the significance between experimental groups. Statistical significance was designated as $p < 0.05$. All experiments were repeated independently for at least three times. Data were presented as mean ± SEM.

3. Results and discussion

3.1. Light mediated gelation and degradation

To date, the gelation mechanisms employed for synthesizing photodegradable hydrogels include a variety of chemistries but not photopolymerization. We reason that photodegradable hydrogels can be easily prepared from photopolymerization if appropriate light sources, macromers, and photoinitiator species are available. As shown in Scheme 1A, our photodegradable hydrogels were prepared from a macromer PEG4NB and a model photodegradable peptide CGOGC. The photo-crosslinking of this step-growth hydrogel was achieved by a visible light-mediated thiol-ene photo-click reaction [24]. In this proof-of-principle work, we selected a commercially available photolabile amino acid (Fmoc-2-NPA) compatible with Fmoc-based solid phase peptide synthesis (SPPS) and incorporated it in the backbone of the model peptide cross-linker CGOGC (Scheme 1B). To achieve rapid gelation, macromer PEG4NB, photolabile peptide cross-linker, and photoinitiator (LAP or EY) were mixed and exposed under a visible light source (400–700 nm).

While visible light-mediated gelation has been used to synthesize hydrogels for biomedical applications for years, all of the conventional visible light gelation systems have focused on cross-linking of vinyl monomers (e.g., PEG-diacrylate (PEGDA) or other (meth)acrylated macromers) with a chain-growth photopolymerization mechanism [28–33]. These cross-linking schemes typically require the use of a co-initiator (e.g., triethanolamine, TEOA) and a co-monomer (e.g., N-vinylpyrrolidone, NVP) to generate sufficient radical species for rapid gelation. In the thiol-ene photopolymerization scheme reported here, cysteine-bearing peptide serves not only as a hydrogel cross-linker, but also as a co-initiator to provide thiyl radicals necessary for initiating thiol-ene photo-click reaction. No co-monomer or other co-initiator is required in this gelation mechanism, which greatly simplifies the preparation of macromer precursor solution. The peptide cross-linker used in this study contains a photolabile amino acid, L-2-NPA. Our main rationale of using this photolabile group was because of its commercial availability, as well as its known photolysis mechanisms [34]. Peters et al. have shown that photolysis of acetylated peptides containing 2-NPA leads to the cleavage of peptide backbone and produces a C-terminal carboxylate group and an N-terminal cinnoline group (Scheme 1C) [34]. It is worth noting that other photo-sensitive motifs (e.g., *o*-nitrobenzyl groups) could also be used to achieve UV-mediated photocleavage.

3.2. Compatibility of photolabile peptides containing 2-NPA with visible light initiators

The synthesis of model photopolymerizable and photolabile peptide CGOGC was achieved using a microwave-assisted peptide synthesizer with high purity (Fig. 1). In order to evaluate the compatibility of this photolabile group with our visible light-mediated thiol-ene gelation, we characterized the absorbance spectrum of the peptide CGOGC and compared it to the spectra of photoinitiators EY and LAP. As shown in Fig. 2A, this photolabile peptide absorbs light only in the UV-range ($\lambda < 400$ nm) and its absorbance peaked at ~290 nm. More importantly, the absorbance spectrum of CGOGC peptide does not overlap with EY's absorbance at wavelengths in the visible light range (400–700 nm), which peaks at ~516 nm. This suggests that EY-mediated thiol-ene photopolymerization should be compatible with the use of this model

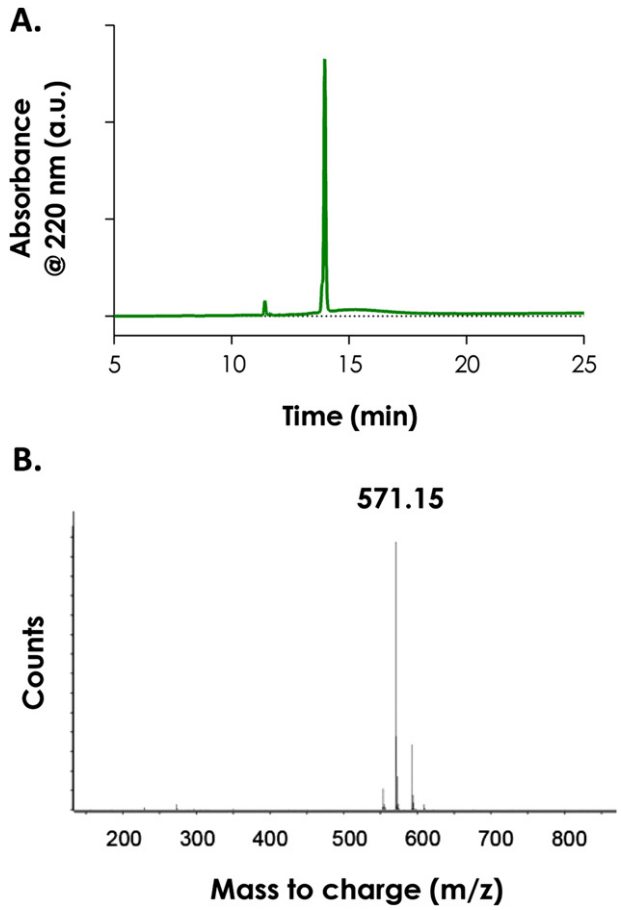

Fig. 1. (A) HPLC trace of purified photodegradable peptide Ac-CGOGC-NH_2. (B) Mass-spec result of purified photodegradable peptide (peptide expected exact mass: 571.15 Da).

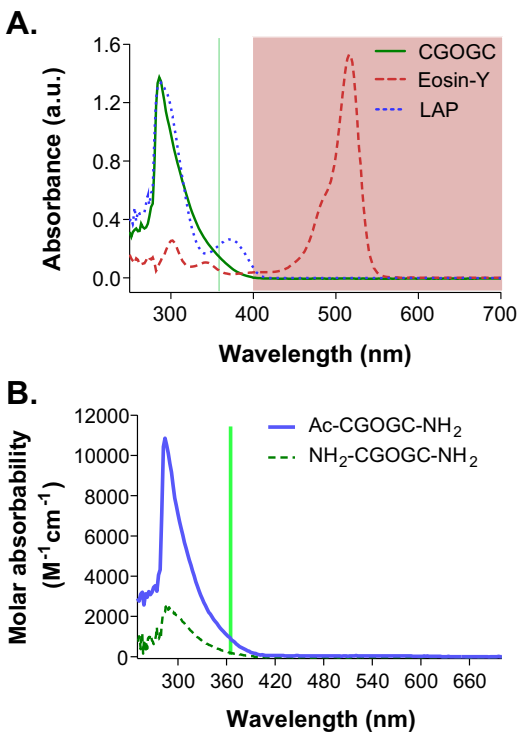

Fig. 2. (A) UV/Vis absorbance spectra of photodegradable peptide, visible light initiator eosin-Y, and UV light initiator LAP (Shaded area indicates visible light absorbance range). (B) Effect of peptide N-terminal acetylation on molar absorbability measured in 10% (v/v) DMSO aqueous solution. Vertical line indicates a wavelength (365 nm) commonly used for UV-mediated reactions.

photolabile peptide. In fact, the molar absorbability of EY in the visible light range is exceptionally high (e.g., $\varepsilon_{516nm} \approx 1 \times 10^5\ M^{-1}\ cm^{-1}$), which makes it suitable for fabricating UV-sensitive photodegradable hydrogels. On the other hand, the spectrum of CGOGC overlaps to a great extent (below 350 nm) with that of lithium arylphosphinate (LAP), a photoinitiator reported by Fairbanks et al. for photopolymerization of vinyl-based hydrogels [26]. Apparently, using UV light to initiate LAP-mediated photopolymerization will result in photolysis, at least partially, of any UV-sensitive photolabile motifs with overlapping UV absorbance. LAP, however, could still be used as a visible light initiator since it absorbs visible light very weakly at 405 nm ($\varepsilon_{405nm} \approx 20\ M^{-1}\ cm^{-1}$).

3.3. Characterization of photolabile peptides containing 2-NPA

A prior report has elucidated the photolysis mechanism for peptides containing 2-NPA [34]. Peptide N-terminal acetylation leads to two major photolysis fragments by restraining additional chemical reactions between the free N-terminal amine group and the nitrophenyl moiety (Scheme 1C). The influence of N-terminal acetylation on the spectrophotometric properties of photolabile peptides, however, has not been examined. Here, we compared the UV/Vis absorbance spectra of CGOGC peptides, either with an unmodified or with an acetylated N-terminus. While both peptides (NH_2-CGOGC-NH_2 and Ac-CGOGC-NH_2) have similar absorption characteristics, the absorbability of Ac-CGOGC-NH_2 in the UV range is much higher than that of NH_2-CGOGC-NH_2 (Fig. 2B). The molar absorbability of Ac-CGOGC-NH_2 at 365 nm was 5-fold higher than NH_2-CGOGC-NH_2 ($\sim$950 vs. $\sim$190 $M^{-1}\ cm^{-1}$), suggesting that Ac-CGOGC-NH_2 was likely more sensitive to UV-mediated photolysis. On the other hand, the molar absorbability of a non-photosensitive peptide, NH_2-CGGGC-NH_2, was very low compared to peptides containing 2-NPA group (Fig. S1).

To assess the photodegradability of the model photolabile peptide, we prepared Ac-CGOGC-NH_2 in 10% DMSO and exposed the peptide solution under 365 nm UV light with an intensity of 10 mW/cm^2 for 1–20 min. As shown in Fig. 3A, the peptide solution was colorless prior to UV light exposure. However, peptide solution became turbid following UV light exposure (Fig. 3A), evidenced by the increase in solution turbidity (Fig. 3B). This was likely due to the production of an aromatic and hydrophobic cinnoline group in the degradation products, which caused small precipitates in the solution. Photodegraded peptides were further characterized by analytical RP-HPLC (Fig. 3C, intact peptide elution time at $\sim$14 min) and ^{1}H NMR (Fig. S3). While the concentrations of the intact peptide decreased following UV light exposure, no desired degraded peptide fragments were identified from mass-spec characterization using samples collected by preparative RP-HPLC (data not shown). The degraded peptide fragments likely formed small precipitates (Fig. 3A) and were filtered off prior to injection into the HPLC column. While ^{1}H NMR was performed in an attempt to identify the degradation products (prior to HPLC analysis), the presence of small precipitates and/or other unknown degradation mechanisms hindered the assignment of protons from the ^{1}H NMR spectra. Nevertheless, a prior study has shown that the degraded peptide fragments react easily with unprotected amine groups [34]. Similar reactions may occur with the added cysteine residues on our model peptides.

From the HPLC results, the areas under the intact peptide peaks ($\sim$14 min) were integrated to obtain concentrations of the intact

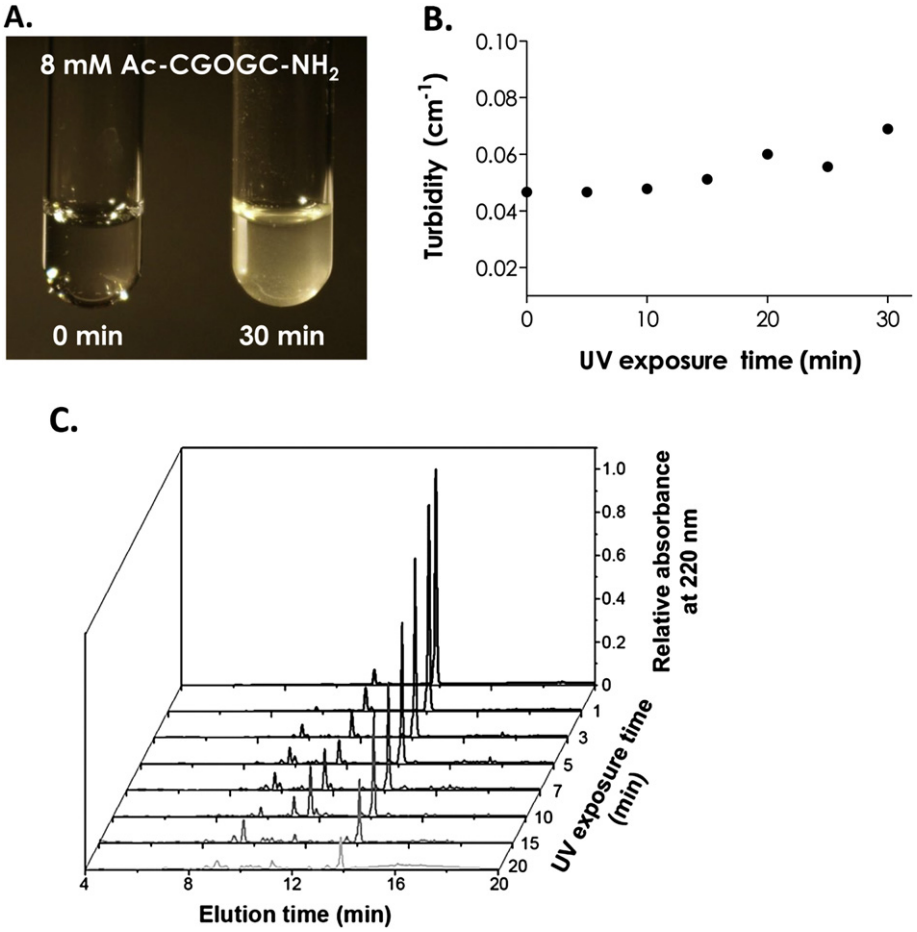

Fig. 3. (A) Photographs of Ac-CGOGC-NH_2 peptide solution prior to and after UV exposure (365 nm, 10 mW/cm^2). (B) Turbidity of Ac-CGOGC-NH_2 peptide solution as a function of UV exposure time (Ac-CGOGC-NH_2 peptide concentration was 8 mM in 10% DMSO). (C) Analytical RP-HPLC traces of photodegraded Ac-CGOGC-NH_2 peptide (C_0 = 0.1 mg/mL) under UV light exposure (365 nm, 10 mW/cm^2). Intact peptide elution time: ~14 min.

peptide after photolysis. As shown in Fig. 4A, concentrations of the photolabile Ac-CGOGC-NH_2 peptide decreased as a function of photodegradation time and only about 20% of the peptide remained intact after 20 min of UV exposure (365 nm, 10 mW/cm^2). The photolysis of this peptide follows a first-order degradation kinetics, which can be expressed as [1]:

$$\frac{C}{C_0} = e^{-kt} \tag{1}$$

Here, C and C_0 are the concentrations of photolabile peptide at any time t during and prior to photodegradation, respectively. k is the photolysis kinetic constant, which can be written as:

$$k = \frac{\varphi \varepsilon I}{N_A h v} \tag{2}$$

Where φ is the quantum yield of the photolabile NPA group (0.07) [34], ε is the molar absorbability of the photolabile peptide (950 M^{-1} cm^{-1}, Fig. 2B), I is the light intensity (10 mW/cm^2), h is Planck constant (6.63×10^{-34} J s), and v is the frequency of light at 365 nm (8.22×10^{14} s^{-1}). For I = 10 mW/cm^2, a photolysis kinetic constant (k) of 2.03×10^{-3} s^{-1} was obtained using Eq. (2).

Using Eqs. (1) and (2), one could easily predict the rate of peptide photolysis (solid curve, Fig. 4A). While the prediction generally agrees with the experimental results determined by HPLC for the first 7 min, the experimental results deviate from prediction for longer exposure time. Further analysis using a semi-log plot revealed that the experimental photolysis kinetic rate constant was 1.57×10^{-3} s^{-1} or 77.3% slower than the model prediction (Fig. S4). This phenomenon was likely a result of light attenuation caused by the aromatic cinnoline groups in the degradation products (Fig. 3A). It is likely that the accumulation of peptide fragments containing cinnoline groups impeded light absorption by the remaining photolabile groups, hence slowing down photolysis rate.

Peptide photolysis could also be achieved by controlling UV light intensity. Combining Eqs. (1) and (2), a relationship between fraction of the intact peptide (C/C_0) and light intensity (I) is obtained:

$$\frac{C}{C_0} = e^{-\frac{\varphi \varepsilon t}{N_A h v} I} \tag{3}$$

Fig. 4B shows a comparison of experimental results and prediction using Eq. (3) with a UV irradiation time of 10 min. While the trend of peptide photolysis at different light intensities (10–40 mW/cm^2) generally agreed with the prediction, there was a slight overestimation of peptide photolysis, especially at lower intensities (e.g., 10 mW/cm^2). This discrepancy could also be explained by the accumulation of cinnoline-bearing fragments that caused light attenuation. At higher light intensities, peptide photolysis occurs more rapidly and the effect of light attenuation caused by the light-absorbing degradation products becomes less prominent.

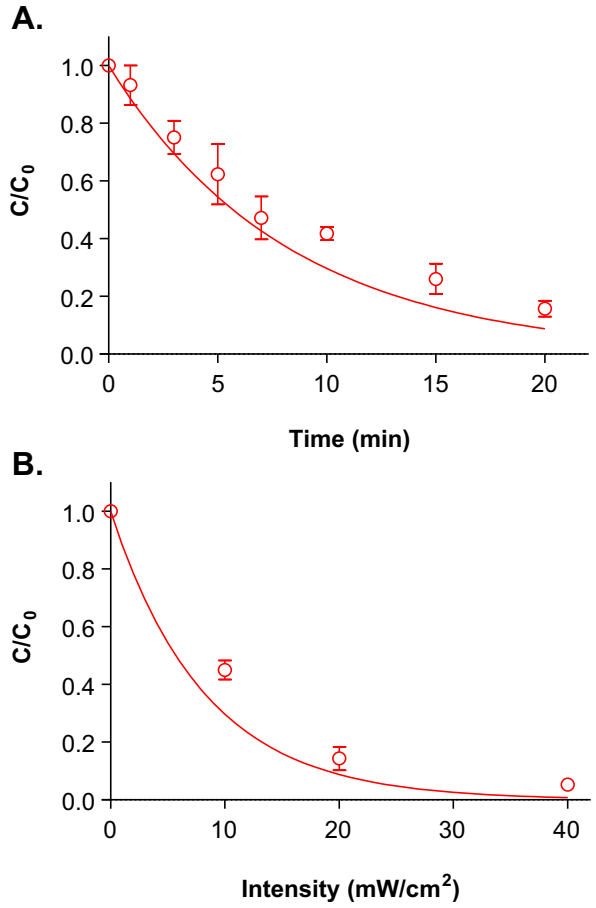

Fig. 4. (A) Effect of UV irradiation time (365 nm, 10 mW/cm^2) on peptide photolysis. Symbols represent experimental results while the exponential decay curve is a prediction using Eqs. (1) and (2). (B) Effect of UV light intensity (365 nm, 10 min) on peptide photolysis. Symbols represent experimental results while the exponential decay curve is a prediction using Eq. (3).

It is worth noting that the acetylated photodegradable peptide (Ac-CGOGC-NH_2) degraded faster than the amine-terminated peptide (NH_2-CGOGC-NH_2). For example, at 20 mW/cm^2 of UV light exposure for 10 min, the concentration of residual amine-terminated CGOGC was about 40% (Fig. S2B) while that of acetylated CGOGC was less than 20% (Fig. 4B). These results show that peptide N-terminal acetylation accelerated photolysis, although the exact mechanisms are not clear. One potential cause for this is the various by-products produced by photolysis of amine-terminated peptides (Fig. S2A). These by-products may compete with the intact peptides on light absorption, therefore decreasing the photolysis rate of amine-terminated peptide. Since acetylated peptides contained less soluble photolysis products (as shown in Fig. 3), light energy could be used more efficiently in peptide photolysis.

While the photolysis of Ac-CGOGC-NH_2 could be readily controlled by altering the dosage of UV light exposure, the photodegradation kinetics (2.03×10^{-3} s^{-1}) of 2-NPA containing peptides appeared to be slower than most of other *o*-NB-containing linkers reported in the literature. This is likely due to a much lower molar absorbability of the 2-NPA containing peptides. For example, the molar absorbability of a photolabile PEG cross-linker with two *o*-NB groups reported by Kloxin et al. was ~7600 M^{-1} cm^{-1} at 365 nm [1]. In another example, DeForest and Anseth reported a photolabile peptide linker containing one *o*-NB group with a molar absorbability of ~5200 M^{-1} cm^{-1} at 365 nm [21]. Although the model peptides used in this proof-of-concept work have a much lower molar absorbability (~950 M^{-1} cm^{-1}), these peptides have zero absorbance in the visible light range that makes it a suitable candidate for visible light-mediated thiol-ene gelation. It is worth noting that peptide linkers containing other *o*-NB groups with higher molar absorbability could certainly be used to increase their susceptibility of UV-mediated photolysis.

3.4. Photopolymerization of photodegradable hydrogels

A highly efficient visible light-mediated thiol-ene photo-click reaction was used to fabricate photodegradable hydrogels. Low concentration of EY (0.1 mM) was used as a type II photoinitiator (or photosensitizer) to initiate thiol-ene photo-crosslinking between PEG4NB and model photolabile peptide NH_2-CGOGC-NH_2. Cysteine residues at the peptide termini serve as proton-donors that, upon visible light exposure, react with the norbornene moieties to form thiol-ether linkages [25]. Gelation kinetics was characterized using *in situ* photo-rheometry. As shown in Fig. 5A, the gelation of PEG4NB-CGOGC hydrogels was rapid and near completion after only 5 min of non-collimated visible light exposure (400–700 nm, 70,000 Lux). In addition to EY, a type I (cleavage-type) photoinitiator LAP was also used to cross-link thiol-ene hydrogels using the same light source (Fig. 5B). A 10-fold higher concentration of LAP (1 mM) was intentionally used due to extremely low molar absorbance of LAP at wavelengths higher than 400 nm (Fig. 2A). However, even with the use of a higher LAP concentration, thiol-ene gelation was much slower compared to using EY at a lower concentration (i.e., 0.1 mM). In addition to the photolabile CGOGC peptide, a control peptide not sensitive to UV cleavage (i.e., CGGGC) was tested for comparison. As shown in Fig. 5C and D, gelation using 0.1 mM EY was again much faster than using 1 mM LAP. Interestingly, when a photosensitive CGOGC peptide was used as PEG4NB hydrogel cross-linker, the gelation rates were faster than using a non-photosensitive peptide (CGGGC) cross-linker regardless of the initiator used (comparing Fig. 5A and C, as well as 5B and 5D). Specifically, the gel point for LAP initiated thiol-ene gelation was roughly 1.4-fold (for CGOGC peptide) to 1.8-fold (for CGGGC peptide) longer than EY initiated thiol-ene gelation (Fig. 6). When comparing gelation using 0.1 mM EY, the gel point for using CGOGC was 3.3-fold faster than using CGGGC. In addition, gelation with LAP was not complete even after 15 min of visible light exposure (Fig. 5B and D).

The major implication of *in situ* photo-rheometry study presented here is that the use of a UV-sensitive photolabile peptide cross-linker does not interfere with visible light-mediated hydrogel cross-linking. In fact, nitrophenylalanine-containing peptides accelerated visible light mediated thiol-ene gelation. We postulated that the presence of 2-NPA group alters the visible light-mediated thiol-ene photoinitiation steps. Further study, however, is required to elucidate the underlying mechanisms, as well as to examine whether this phenomenon still occurs when the nitrophenylalanine residue is replaced by other *o*-NB moiety. Nonetheless, these studies demonstrated the feasibility and effectiveness of using EY-mediated thiol-ene photopolymerization to rapidly fabricate photodegradable hydrogels without using cytotoxic components.

3.5. Photodegradation of photopolymerized hydrogels

To further demonstrate the feasibility of these photopolymerized hydrogels to undergo photodegradation, a proof-of-concept photodegradation experiment with flood UV irradiation was performed. Fig. 7(A) shows PEG4NB-CGOGC hydrogels (8 wt%) prior to and after UV light (365 nm, 10 or 20 mW/cm^2) exposure for 30 min. Clearly, both the volume and diameter of gel discs exposed

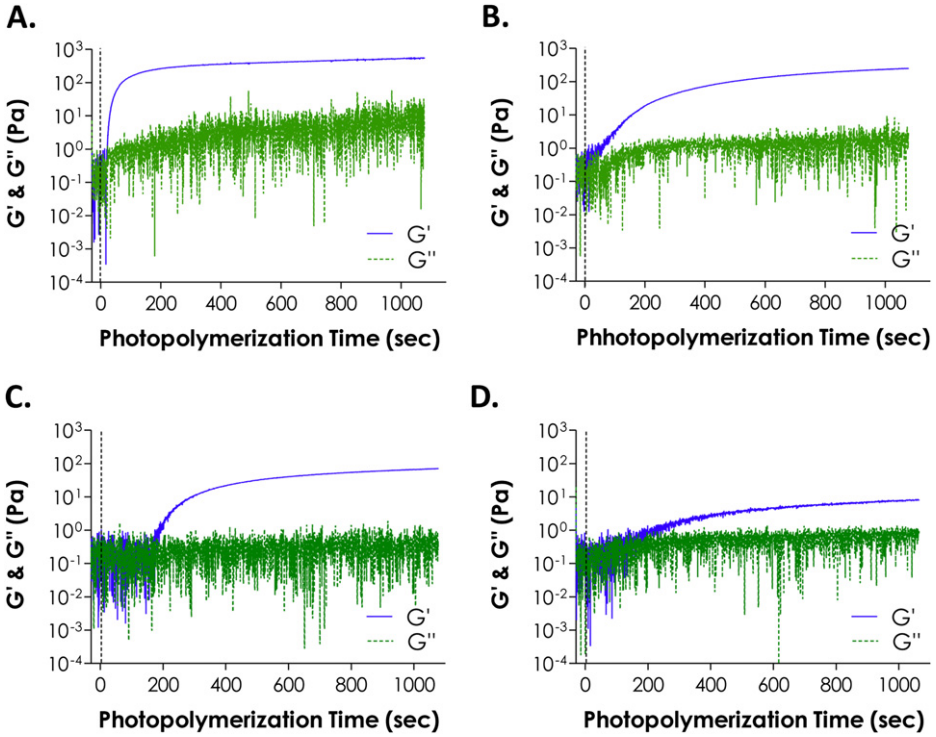

Fig. 5. Evolution of storage (G′) and loss (G″) moduli during visible light-mediated photopolymerization of photodegradable PEG hydrogels (Light wavelength: 400–700 nm. Light intensity: 70,000 Lux. PEG4NB: 5 wt%). (A & B): Cross-linked by NH_2-CGOGC-NH_2 using (A) 0.1 mM eosin-Y or (B) 1 mM LAP as the photoinitiator. (C & D): Cross-linked by NH_2-CGGGC-NH_2 using (C) 0.1 mM eosin-Y or (D) 1 mM LAP as the photoinitiator.

to flood UV light decreased due to photo-erosion. Another indication of photodegradation is the change of gel color after UV light exposure. Similar to the cleavage of soluble peptide (Fig. 3A), the color of the hydrogel changed from transparent to yellowish. It was likely that the newly formed aromatic cinnoline group-containing degradation products were trapped with the degrading gel network and caused the color change (Scheme 1C).

Fig. 7B shows the mass loss profiles of these photodegradable hydrogels. In addition to the commonly used 365 nm light, a shorter wavelength (302 nm) of UV light was also used to examine the gel erosion kinetics. UV light at 302 nm was used because the model photolabile peptide cross-linker CGOGC absorbs light strongly between 290 nm and 310 nm (Fig. 2). As shown in Fig. 7B, the mass loss profile of gel photo-erosion using 302 nm light

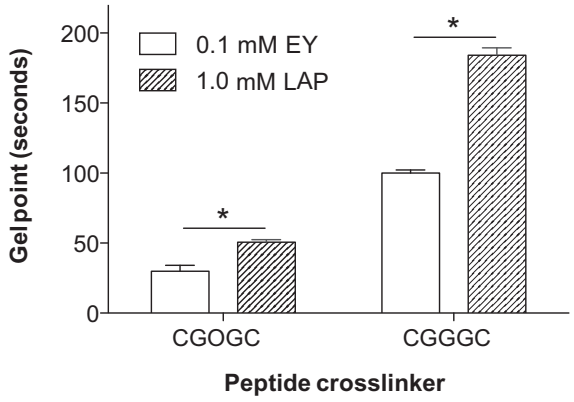

Fig. 6. Gel points of photodegradable hydrogels determined by *in situ* photorheometry ($N = 3$, mean ± SEM). Asterisks indicate $p < 0.05$ between the indicated groups.

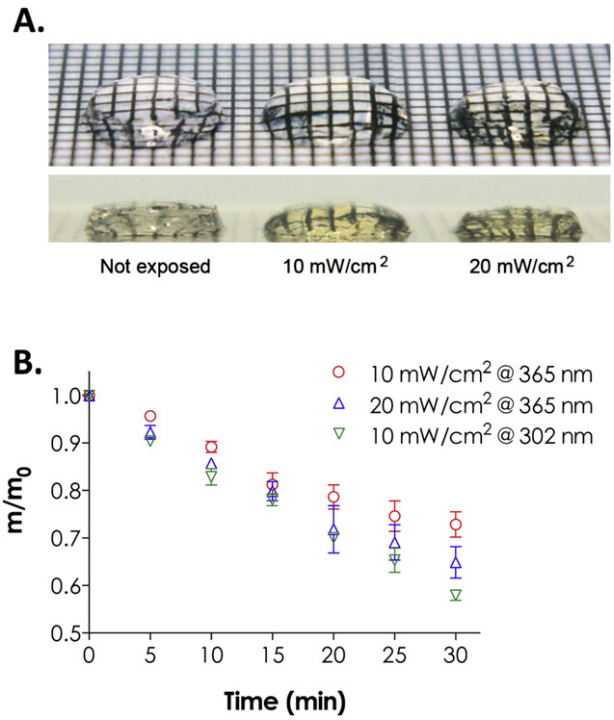

Fig. 7. (A) Photographs of photodegraded hydrogels (8 wt% of PEG4NB cross-linked by Ac-CGOGC-NH_2). The hydrogels were exposed to UV light (365 nm) of different intensities for 30 min. Grid gap is 1 mm. (B) Effect of different wavelength UV lights (302 or 365 nm, 10 mW/cm^2) on reduction of residual hydrogel mass ($N = 3$, mean ± SEM).

appears to decrease linearly during the 30-min photodegradation test (linear regression $R^2 > 0.99$). Although these gels were also degraded by 365 nm light, the rate of photo-erosion at this UV wavelength decreased as time for both intensities tested (10 and 20 mW/cm^2). Specifically, the rates of gel erosion in the first 15–20 min were faster and more linear compared to the erosion rates after light exposure for 20 min. A recent study by Kloxin et al. using step-growth azide-cyclooctyne-based photodegradable hydrogels also showed a non-linear photo-erosion rate at longer UV irradiation time [35]. The non-linear monotonic decrease in gel mass was likely a combinatorial result of light attenuation, diffusion of the degradation products away from the gel surface, and photodegradation. Controlled experiments using non-photosensitive peptides (e.g., CGGGC and CGGYC) showed no reduction in gel mass after UV exposure (data not shown).

Although not shown in this contribution, the photopolymerized photodegradable thiol-ene hydrogels reported here should be fully compatible with other attractive features offered by the light mediated thiol-ene photo-click reactions. For example, bioactive motifs can be patterned, in a spatial-temporally controlled manner, on the surface of or within the thiol-ene hydrogels even in the presence of encapsulated cells. DeForest and Anseth have recently reported the use of eosin-Y as a photoinitiator to conjugate thiol-containing peptides on pendent alkene groups in an azide-cyclooctyne-based photodegradable hydrogel [21,36]. The gelation system presented in this contribution should also be fully compatible with the sophisticated bioconjugation techniques reported by DeForest and Anseth due to the post-gelation conjugation ability offered by the thiol-norbornene photochemistry [25]. Furthermore, since none of the reported *o*-NB groups have absorbance at long visible light wavelengths ($\lambda > 450$ nm), the visible light-mediated thiol-ene gelation chemistry demonstrated here should be compatible with many of the photolabile *o*-NB groups, as long as a collimated light source (e.g., at 516 nm, peak absorbance of EY) is used to initiate gel cross-linking. The utility of this photopolymerized photodegradable hydrogel system can be further expanded with the use of bioactive photolabile peptides (e.g., matrix metalloproteinase-sensitive peptides). Finally, light mediated controlled release of biomolecules can also be achieved using this hydrogel platform by tethering drug of interest to the photolabile peptides.

4. Conclusion

In conclusion, we have demonstrated UV-mediated photodegradable hydrogels could be conveniently synthesized via visible light-mediated thiol-ene photopolymerization. The hydrogels were cross-linked by PEG4NB and *bis*-cysteine peptide containing a photolabile moiety (2-NPA) under visible light (400–700 nm) exposure with eosin-Y as an efficient photoinitiator while photodegradation of these gels was achieved by UV light irradiation. This system embraces the power of both thiol-ene photo-click chemistry and light-mediated gel degradation. This system also provides a convenient way of synthesizing photodegradable hydrogels without the use of cytotoxic components. Taken together, this photopolymerization platform represents a simple yet efficient synthesis route to fabricate photodegradable hydrogels for controlled release and tissue engineering applications.

Acknowledgement

This project was supported by a Faculty Start-up Fund from the Department of Biomedical Engineering at IUPUI and the National Institutes of Health (R21EB013717).

Appendix A. Supplementary data

Supplementary data related to this article can be found at http://dx.doi.org/10.1016/j.polymer.2013.02.018.

References

[1] Kloxin AM, Kasko AM, Salinas CN, Anseth KS. Science 2009;324(5923):59–63.
[2] Griffin DR, Patterson JT, Kasko AM. Biotechnol Bioeng 2010;107(6):1012–9.
[3] Griffin DR, Kasko AM. J Am Chem Soc 2012;134(42):17833.
[4] Tibbitt MW, Han BW, Kloxin AM, Anseth KS. J Biomed Mater Res A 2012;100A(7):1647–54.
[5] Griffin DR, Kasko AM. ACS Macro Lett 2012;1(11):1330–4.
[6] Kloxin AM, Tibbitt MW, Kasko AM, Fairbairn JA, Anseth KS. Adv Mater 2010;22(1):61–6.
[7] Kloxin AM, Benton JA, Anseth KS. Biomaterials 2010;31(1):1–8.
[8] Wang H, Haeger SM, Kloxin AM, Leinwand LA, Anseth KS. Plos One 2012;7(7):e39969.
[9] Murayama S, Ishizuka F, Takagi K, Inoda H, Sano A, Santa T, et al. Anal Chem 2012;84(3):1374–9.
[10] Narayanan RP, Melman G, Letourneau NJ, Mendelson NL, Melman A. Biomacromolecules 2012;13(8):2465–71.
[11] Yan B, Boyer JC, Habault D, Branda NR, Zhao Y. J Am Chem Soc 2012;134(40):16558–61.
[12] Fairbanks BD, Singh SP, Bowman CN, Anseth KS. Macromolecules 2011;44(8):2444–50.
[13] Baskin JM, Bertozzi CR. Qsar Comb Sci 2007;26(11–12):1211–9.
[14] Klinger D, Landfester K. Macromolecules 2011;44(24):9758–72.
[15] Klinger D, Landfester K. Soft Matter 2011;7(4):1426–40.
[16] Klinger D, Landfester K. J Polym Sci A Polym 2012;50(6):1062–75.
[17] Temenoff JS, Shin H, Conway DE, Engel PS, Mikos AG. Biomacromolecules 2003;4(6):1605–13.
[18] Shih H, Lin CC. Biomacromolecules 2012;13(7):2003–12.
[19] Peng K, Tomatsu I, van den Broek B, Cui C, Korobko AV, van Noort J, et al. Soft Matter 2011;7(10):4881–7.
[20] Metters A, Hubbell J. Biomacromolecules 2005;6(1):290–301.
[21] DeForest CA, Anseth KS. Nat Chem 2011;3(12):925–31.
[22] Baskin JM, Prescher JA, Laughlin ST, Agard NJ, Chang PV, Miller IA, et al. P Natl Acad Sci USA 2007;104(43):16793–7.
[23] Chang PV, Prescher JA, Sletten EM, Baskin JM, Miller IA, Agard NJ, et al. P Natl Acad Sci USA 2010;107(5):1821–6.
[24] Shih H, Lin CC. Macromol Rapid Commun 2013;34(3):269–73.
[25] Fairbanks BD, Schwartz MP, Halevi AE, Nuttelman CR, Bowman CN, Anseth KS. Adv Mater 2009;21(48):5005–10.
[26] Fairbanks BD, Schwartz MP, Bowman CN, Anseth KS. Biomaterials 2009;30(35):6702–7.
[27] Ki CS, Lee KH, Baek DH, Hattori M, Um IC, Ihm DW, et al. J Appl Polym Sci 2007;105:1605–10.
[28] Hu J, Hou Y, Park H, Choi B, Hou S, Chung A, et al. Acta Biomater 2012;8(5):1730–8.
[29] Kizilel S, Sawardecker E, Teymour F, Perez-Luna VH. Biomaterials 2006;27(8):1209–15.
[30] Sawhney AS, Pathak CP, Hubbell JA. Biomaterials 1993;14(13):1008–16.
[31] Cruise GM, Hegre OD, Scharp DS, Hubbell JA. Biotechnol Bioeng 1998;57(6):655–65.
[32] Bahney CS, Lujan TJ, Hsu CW, Bottlang M, West JL, Johnstone B. Eur Cells Mater 2011;22:43–55.
[33] Kim SH, Chu CC. Fiber Polym 2009;10(1):14–20.
[34] Peters FB, Brock A, Wang J, Schultz PG. Chem Biol 2009;16(2):148–52.
[35] Kloxin AM, Lewis KJR, DeForest CA, Seedorf G, Tibbitt MW, Balasubramaniam V, et al. Integr Biol 2012;4(12):1540–9.
[36] DeForest CA, Anseth KS. Angew Chem Int Ed 2012;51(8):1816–9.

Facile preparation of photodegradable hydrogels by photopolymerization

Chang Seok Ki, Han Shih, and Chien-Chi Lin*

Department of Biomedical Engineering,
Purdue School of Engineering and Technology,
Indiana University-Purdue University at Indianapolis, Indianapolis, IN 46202 USA

(Supporting Figures)

*To whom correspondence should be addressed:
Chien-Chi Lin, PhD.
Assistant Professor
Department of Biomedical Engineering
Purdue School of Engineering and Technology
Indiana University-Purdue University at Indianapolis
Indianapolis, IN 46202
Email: lincc@iupui.edu

Supporting Figures

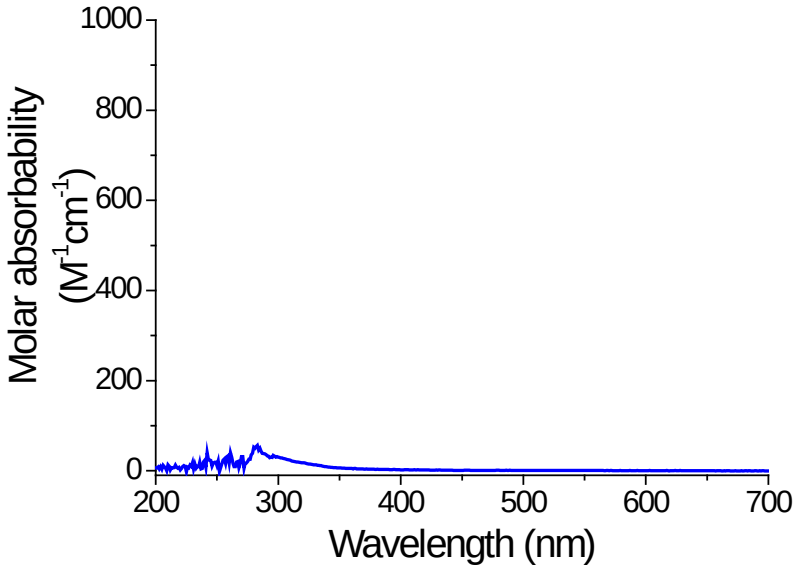

Fig. S1. UV/Vis spectrum of H_2N-CGGGC-NH_2.

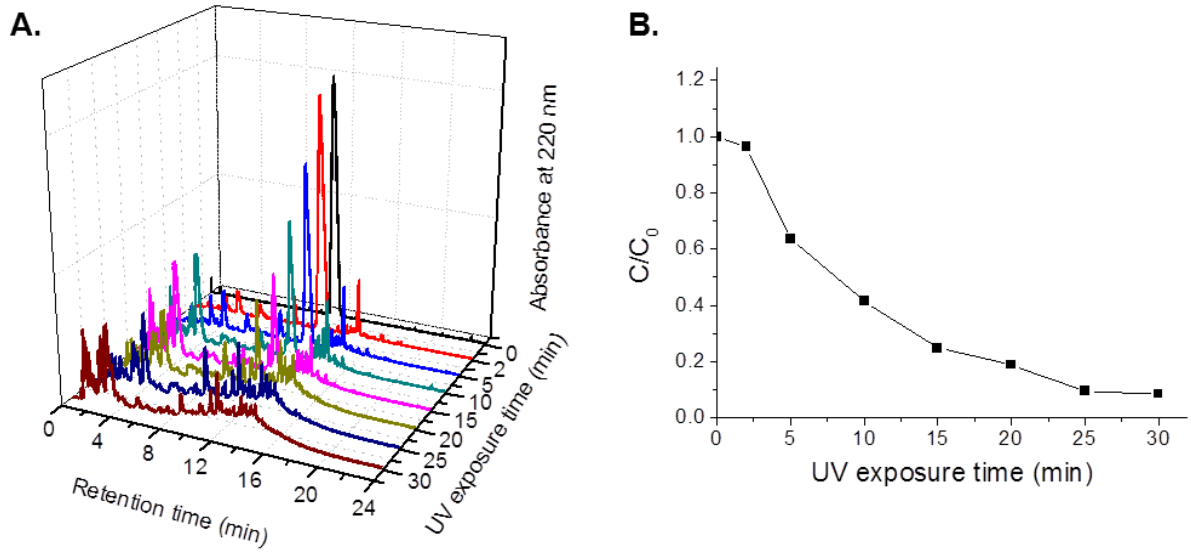

Fig. S2. (A) HPLC traces of photo-cleaved H_2N-CGOGC-NH_2 (B) Concentration of intact peptide (elution time ~13min) normalized to C_0 (intact peptide concentration prior to photocleavage). UV irradiation condition was 20 mW/cm^2 at 365 nm.

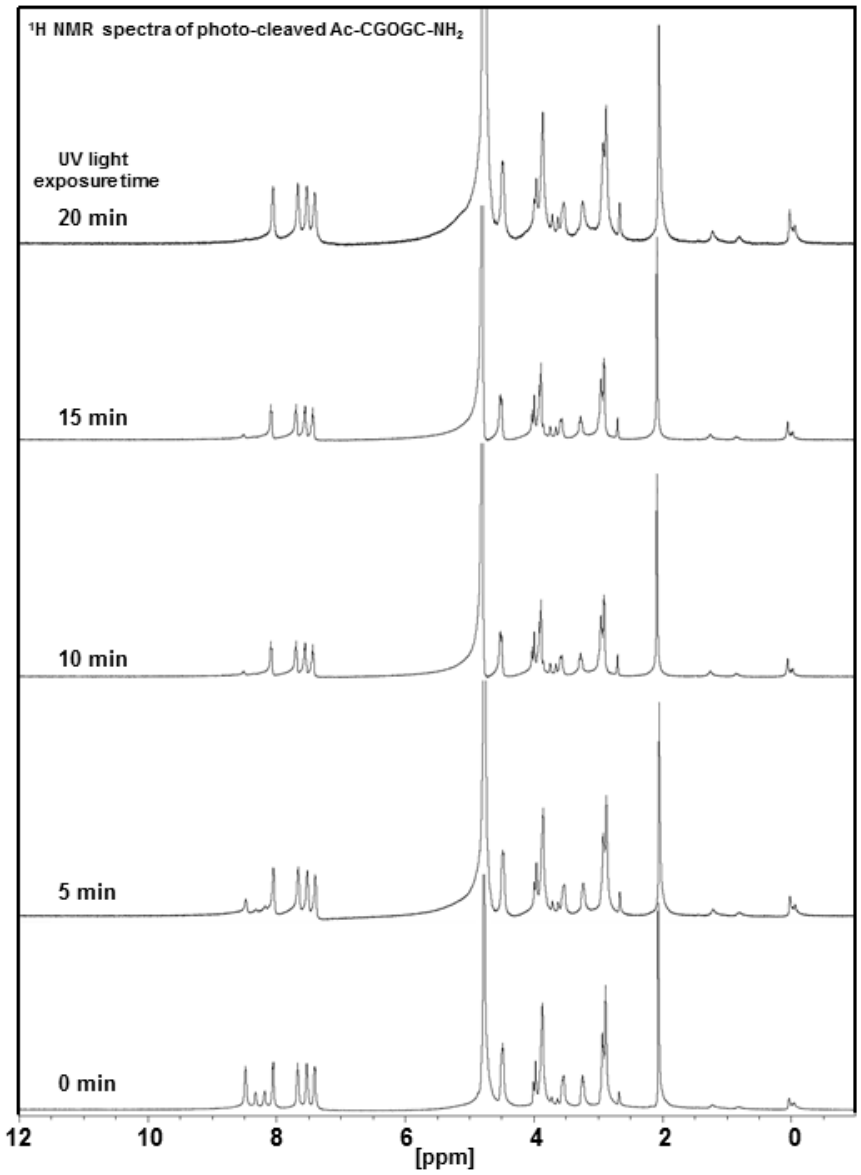

Fig. S3. ^{1}H NMR spectra of photo-cleaved Ac-CGOGC-NH_2 dissolved in 10% dimethyl sulfoxide-d6/90% deuterium oxide. The solution was exposed to UV light (10 mW/cm^2, 365 nm) and detected at 5 min intervals.

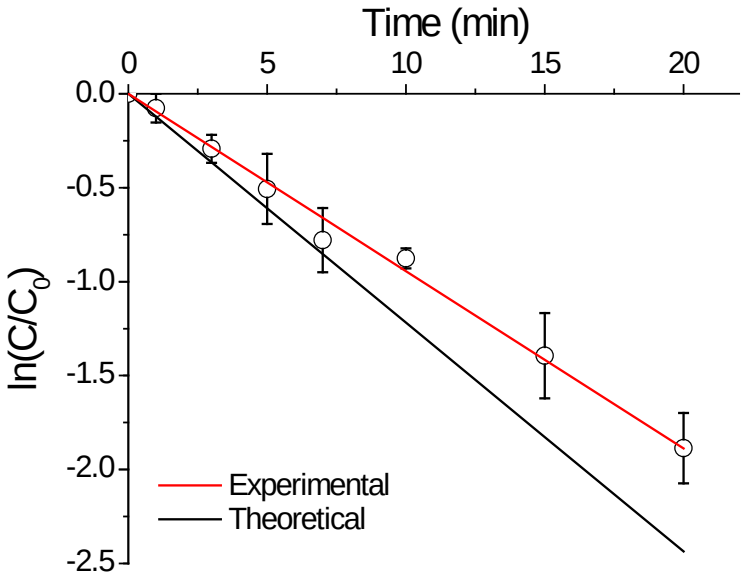

Fig. S4. Effect of UV (365 nm, 10 mW/cm^2) irradiation time on Ac-CGOGC-NH_2 photolysis. Red and black solid lines indicate linear fitting results of experimental values and theoretical values (calculated using Eqs. 1 and 2), respectively. The experimentally obtained photolysis kinetic constant (k) was 1.57×10^{-3} s^{-1} while the theoretical value was 2.03×10^{-3} s^{-1}.